Tin clusters adopt prolate geometries

Alexandre A. Shvartsburg and Martin F. Jarrold
Department of Chemistry, Northwestern University, 2145 Sheridan Road, Evansion, Illinois 60208
(Received 16 February 1999)

We have characterized the structures of Sn_n cations up to $n=68$ using ion mobility measurements. Up to $n\sim35$, tin clusters track the prolate growth pattern previously found for Si_n and Ge_n. However, the detailed size-dependent variations start deviating from those observed for Si_n above $n=14$ and Ge_n above $n=21$. Over the $n\sim35-65$ size range, tin clusters gradually rearrange towards near-spherical geometries, passing through several intermediate structural families. Two or three isomers are resolved for some sizes in the $n=18-49$ range. The observed geometries are independent of the He buffer gas temperature between 78 and 378 K and are not affected by collisional annealing. [S1050-2947(99)02608-6]

PACS number(s): 36.40.Mr, 36.40.Ei, 36.40.Wa

Over the last decade, the structural elucidation of free atomic clusters has been an area of intense research effort. Most elements evolve from just a few atoms to nanoparticles simply by sequentially accruing new layers of atoms. These layers may form atomic (geometric) shells, such as in clusters of noble gas atoms [1], alkaline earths [2], and some transition metals, including Ni, Fe, and Co [3–8]. In clusters with atomic shells, these layers arrange to produce an ordered packing of hard spheres, most often icosahedral. The clusters of free electron metals with weakly directional bonding normally adopt an electronic shell structure, where the geometry adapts to minimize the total electronic energy. This is characteristic of the alkali [1,9] and coinage [1] metals, and group 13 elements (aluminum [10,11], gallium [12], indium [13], and thallium [14]). Species of group 12 metals (zinc, cadmium, and mercury) undergo a transition to the electronic shell structure once the *s* and *p* electrons are hybridized [15]. Obviously, the clusters of all elements must eventually assume the bulklike structure [16]. The dominance of geometric or electronic shell structure for a particular cluster may also depend on the temperature [17]. In any case, most elements *including all previously studied metals* form densely packed clusters that grow without gross deviations from near-spherical shape.

The only species found to assume noncompact geometries and thus experience major structural transitions are those of covalently bound nonmetals, in particular the group 14 elements: carbon [18], silicon [19,20], and germanium [21]. Carbon clusters undergo an especially colorful progression of rearrangements: from linear chains to monocyclic rings to polycyclic rings to graphite sheets to fullerenes [18]. Clusters of Si and Ge first grow in one dimension forming prolate structures, but then abruptly rearrange to more spherical geometries once the clusters contain several dozen atoms [19–21]. It has recently been shown that the prolate sequence for Si_n is built by stacking exceptionally stable Si_9 tricapped trigonal prism units [22–24]. Some similarities exist between the growth patterns of Si and Ge clusters. There are also major differences, in particular in the size range where the transition to more compact geometries occurs. Tin is immediately below germanium in the periodic table. Its normal allotrope under ambient conditions (white or β-Sn) is a typical metal with a body-centered tetragonal lattice, but it also has a semiconductor form (gray or α-Sn) that is thermodynamically preferred below 286 K [25]. Crystalline α-Sn has the same tetrahedral ''diamond'' lattice as Si and Ge. No other element has stable solid metallic and semiconducting phases, unless under ultrahigh pressure. This renders the investigation of tin clusters to be of great interest.

Very little is known about tin clusters with more than just a few atoms from either experiment or calculations. Thermochemical quantities for the smallest ($n\leqslant7$) Sn_n neutrals have been determined by third-law measurements [26]. The mass spectrum of Sn_n cations produced by the ionization of condensed elemental vapor was found to resemble that of Pb_n^+, but not that of Ge_n^+ [27]. This was thought to indicate the metallic rather than semiconductor nature of tin clusters [27,28]. Specifically, the abundance minimum at $n=14$ was interpreted as evidence for compact structures (with a complete geometric shell of atoms closing at $n=13$ making a perfect icosahedron). On the other hand, the mass spectra of Sn_n^+ coming out of a liquid metal ion source [29,30] were almost identical to those of Si_n^+ and Ge_n^+ obtained under the same conditions but different from those of Pb_n^+. For example, $n=4$, 6, and 10 were particularly abundant for silicon, germanium, and tin clusters, while lead ones exhibited no ''magic sizes.'' This has been the basis for conclusion that tin clusters are covalently bound and not metallic [30]. Evidently, the abundance distributions are strongly dependent on precise source conditions and, in general, reveal little about cluster structure. Duncan and co-workers [31] have surveyed the abundance distribution of Sn_n^+ produced by laser vaporization of β-Sn under various conditions and bracketed the ionization potentials for selected neutrals. They concluded that Sn clusters have properties intermediate between those of Ge and Pb, although closer to Pb. In contrast, photoelectron spectra of Sn_n anions obtained by Ganteför *et al.* for $n\leqslant22$ are similar to those of Ge_n^- but not to those for Pb_n^- [32]. This led to a hypothesis that tin clusters in this size range are not metallic. The chemical reactivity of small Sn_n ($n\leqslant9$) anions towards oxygen, nitrous oxide, hydrogen sulfide, methane, and several simple alcohols has been determined [33,34], but this has not yielded any structural inferences.

Several authors [34–37] have optimized the geometries for small Sn_n neutrals and anions using the molecular orbital

theory [35], multiconfiguration complete active space self-consistent-field method followed by multireference singles and doubles configuration interaction (CASSCF/MRSDCI) [36], and density functional theory in the local density approximation (LDA) and with several gradient-corrected functionals [34,37]. The consensus now is that the global minima for neutrals with $n \leqslant 7$ are identical to those previously established for the Si_n [38–40] and Ge_n [41–43] species by photoelectron spectroscopy and IR/Raman spectroscopy in matrix: a triangle for $n=3$, a rhombus for $n=4$, and bicapped trigonal, tetragonal, and pentagonal bipyramids for $n=5$, 6, and 7, respectively. The species in the $n=8-10$ range have recently been optimized by Stott and collaborators using LDA [37]. They found an edge-capped pentagonal bipyramid for Sn_8 and a C_{2v} horizontally bicapped distorted pentagonal bipyramid for Sn_9. These geometries differ from those for Si_n [22,44,45] and Ge_n [43,44], a distorted bicapped octahedron for $n=8$, and the C_{2v} capped Bernal structure for $n=9$. However, Sn_{10} [37] is the tetracapped trigonal prism like Si_{10} and Ge_{10}.

Here we report on the structural characterization of singly charged tin cluster cations with up to 68 atoms using ion mobility measurements. The tandem quadrupole drift tube apparatus used in this work has been described in detail [46]. Briefly, the cluster ions are generated by pulsed 308 nm laser vaporization of a β-tin rod and entrained in a continuous helium flow. They are mass selected and injected in a 20–50 μs wide pulse at a controlled energy into a 7.6 cm long drift tube containing He buffer gas. The clusters exiting the drift tube are mass selected one more time and detected by an off-axis collision dynode and dual microchannel plates. The drift tube can be cooled down to 78 K using liquid nitrogen or heated up to 380 K by electric heaters. The temperature is monitored by five thermocouples installed along the drift tube, and the gradient is below 2 K. The drift field was 15.5 V/cm and the buffer gas pressure was varied in the range of 5–10 Torr. The cluster source can also be cooled down to 78 K by liquid nitrogen. It has been established that the clusters leaving the source are close to its temperature [10].

The mobilities of tin cluster cations measured at 305 K are plotted in Fig. 1, along with the data for Si_n [19,20] and Ge_n [21] cations at room temperature. Only one feature was resolved for each size, although some peaks are substantially broadened and thus presumably encompass several isomers. For selected sizes, measurements were performed as a function of source temperature (78–300 K) and injection energy (50–600 eV). Neither of these factors significantly affected the mobilities, even though many clusters were nearly completely dissociated at the highest injection energies. All results are expressed in terms of relative mobilities $K_{\mathrm{rel}} = K_{\mathrm{expt}}/K_{\mathrm{sph}}$. Here K_{expt} is the mobility measured for an n-atom cluster and K_{sph} is that computed [47] for a fictitious sphere of a volume nV_{at}, where V_{at} is the atomic volume of the bulk element under ambient conditions. This normalization largely removes the systematic variation of mobility with cluster size, allowing one to highlight the evolution of cluster shape as a function of number of atoms. Compact near-spherical isomers have larger relative mobilities, whereas smaller values indicate geometries that substantially deviate from spherical. As reported previously [19,20], Si_n cations undergo a structural transition from stacks of tri-

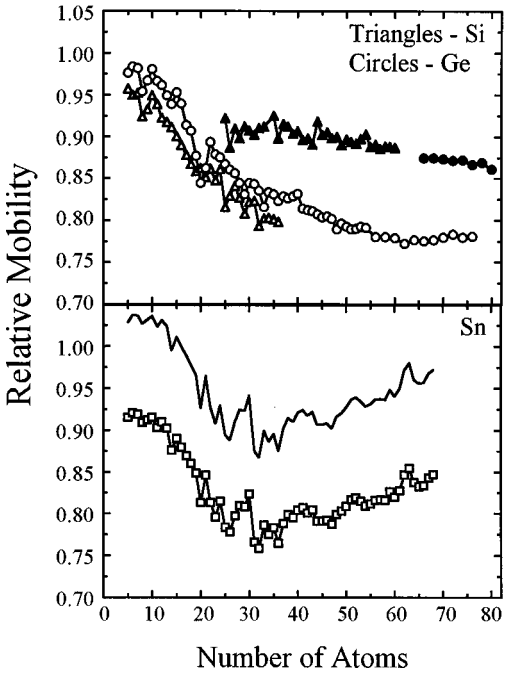

FIG. 1. Relative mobilities of Group 4 cluster cations measured at room temperature. The upper and lower lines for Sn_n^+ correspond respectively to the bulk densities of α- and β-tin. Open and closed symbols for Si and Ge clusters stand for the families before and after the structural transition, respectively.

capped trigonal prisms to cagelike near-spherical geometries in the $n=24-34$ range. This transition can clearly be seen in Fig. 1. A similar transition occurs for Ge_n cations [21,49] between $n=64$ and 76. Importantly, the relative mobilities of the more spherical Si_n and Ge_n isomers fall on one line. This means that the larger Ge clusters are similar in shape to the larger Si_n, which have compact near-spherical geometries [50]. The change in relative mobilities of Si and Ge clusters beyond the structural transition is not primarily structurally related, but caused by multiple scattering [48] and van der Waals interactions of the He atoms with the cluster [51,52]. Both these effects decrease the mobility of any polyatomic ion, but their magnitude uniformly increases with increasing cluster size. Hence the relative mobilities of near-spherical families of Si and Ge clusters (Fig. 1) approximately delineate the position of most compact structures for tin clusters, assuming that the clusters of any element have the same density as the bulk.

It is apparent from Fig. 1 that the mobilities for tin clusters up to $n \sim 35$ closely follow the global trend of germanium and the prolate silicon species. All size-to-size variations are also reproduced for $n<12$. In the $n=12-20$ range, there are prominent local minima in the relative mobilities at $n=14$ and 20 that are strikingly similar to those for Ge_n^+ but absent for Si_n^+. For $n>20$, the mobilities of Sn_n^+ exhibit larger fluctuations than those for both Si_n^+ and Ge_n^+ and are not correlated with either of them qualitatively. This may be caused by the presence of multiple isomers for many Sn_n^+ clusters in this size range, as discussed below. Around $n=35$, the overall trend reverses and the relative mobilities of tin clusters start increasing with increasing size. By $n=68$, they almost reach the level characteristic of the most com-

pact near-spherical objects, assuming the bulk density of β-tin. The atomic volume of crystalline α-tin is larger than that for the β-allotrope by 27%. So, if the measured mobilities of clusters are normalized with respect to the bulk density of α-tin, the K_{rel} values for almost all sizes are substantially above the values expected for near-spherical geometries and exceed unity for small clusters. This is clearly unphysical, thus the typical density of tin clusters throughout the size range studied must be significantly higher than that of bulk α-tin. So at room temperature tin clusters up to $n \sim 35$ are structurally similar to both Si and Ge species. The behavior observed for $n \gtrsim 35$ may either signify the conversion of clusters into the compact balls normally expected for metal nanoparticles or constitute an unrelated structural transition to near-spherical geometries, such as that taking place for Si_n or Ge_n in the similar size ranges. However, the measured densities of tin clusters for $n \gtrsim 60$ match the bulk density of β- and not α-tin assuming that they are close to compact and nearly spherical. Otherwise, the density would be even greater than that of bulk β-tin.

We emphasize that the behavior of tin clusters in the $n \gtrsim 35$ size range is not analogous to the extensively studied nonmetal-to-metal transition in group 12 elements species [15,53–56]. The small clusters of those elements have weak van der Waals bonding because of the closed-shell s^2 electronic configuration that renders the atoms similar to those of noble gases. A nonmetal-to-metal transition refers to the development of metallic bonding through the hybridization of s and p orbitals. In contrast, even the smallest tin clusters are strongly bound [26].

As mentioned above, bulk tin prefers the α form below 286 K. So we have repeated all measurement for $n < 58$ with the buffer gas at 78 K searching for any structural rearrangements [see Fig. 2(a)] [57]. At room temperature, we resolved only one isomer for each size. At 78 K, about a quarter of the clusters in the $n \geqslant 18$ range ($n = 18,21,24,27,37,44,46-49$) have two isomers, and Sn_{30}^+ has three (see Fig. 3). The broad peaks for some other sizes in this range indicate the presence of unresolved isomers. So multiple geometries are separated for every third size in the $n = 16-32$ range, but there is no obvious rule for larger species. It is, however, clear from Fig. 2(a) that the isomer distribution is not random. All clusters fall into a number of distinct families with a new one starting roughly every ten atoms (although our grouping is perhaps somewhat arbitrary). This is intriguing since the tricapped trigonal prism containing nine atoms is the building block of medium-sized silicon [22–24] and germanium [60] clusters.

Multiple isomers may appear at low drift tube temperatures for three reasons: (i) there exist relatively unstable geometries that anneal or dissociate at higher temperatures; (ii) there are isomers with the barriers to interconversion that at higher temperatures are surmountable on the experimental time scale, although the geometries themselves are stable; or (iii) the geometries with a small difference in mobility that are not resolved at higher temperatures are now separated due to the better resolution (the resolution is proportional to the square root of temperature [46]). The comparison of arrival time distributions at two temperatures reveals that multiple isomers appear at 78 K mostly for those sizes that feature broadened peaks at 305 K. Considering that the largest difference in mobility between two neighboring peaks at 78 K is under 6% (for Sn_{47}^+), none of them would be separated at room temperature. This suggests that the appearance of new isomers at low temperatures is not an intrinsic effect of freezing out the local minima, but merely an artifact of enhanced instrumental resolution. To confirm this, we compare the size-dependent variations in average mobilities (weighted by the isomer abundances) measured at 78 K with those measured at 305 K [see Fig. 2(b)]. All features are perfectly

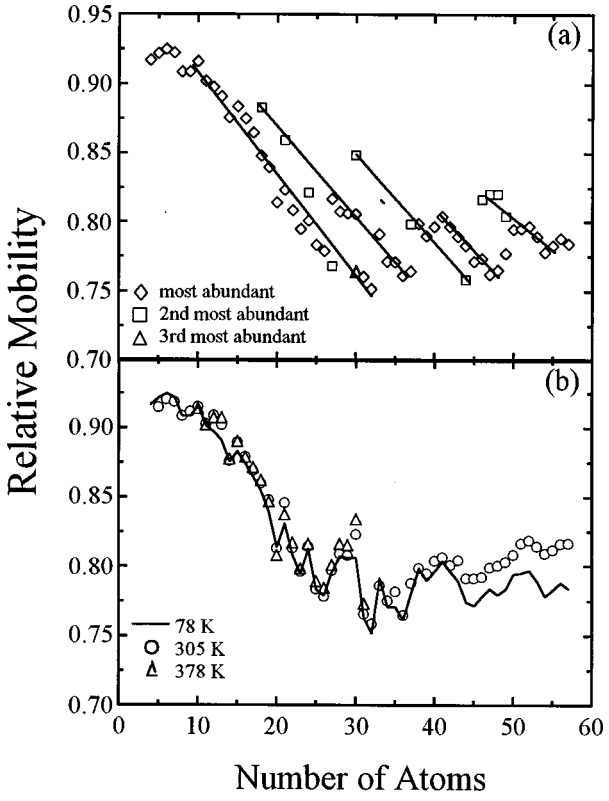

FIG. 2. Relative mobilities of Sn_n^+ isomers measured as a function of buffer gas temperature (assuming the bulk density of β-tin). Straight lines in (a) mark possible structural families. In (b), the curve shows the weighted average of values for all isomers of a particular size observed at 78 K, and the symbols are the data for 305 K (circles) and 378 K (triangles).

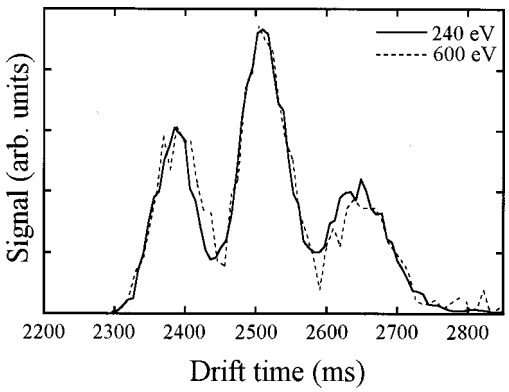

FIG. 3. Drift time distributions measured for Sn_{30}^+ with the drift tube at 78 K reveal three isomers independent of the injection energy. Results are shown for injection energies of 240 and 600 eV.

reproduced, moreover the relative mobilities at two temperatures are equal at least through $n \sim 45$ [61]. Also, the isomer distributions measured at 78 K are not strongly affected by either injection energy or source temperature. This would be implausible if any structures unstable at room temperature were present. Therefore we conclude that the geometries of tin cluster cations do not noticeably change over a wide range of temperatures including the region of $\beta \Rightarrow \alpha$ phase transition in bulk tin.

While the bulk β form is more stable than the α form above 286 K, the $\alpha \Rightarrow \beta$ transformation is quite slow until $\sim$310 K [25]. This makes it important to study tin clusters at higher temperatures, in order to determine if a rearrangement analogous to the bulk transition takes place. So we have measured the mobilities for Sn_n^+ $9 < n < 32$ at 378 K. We have found that every single size-dependent feature is quantitatively reproduced [Fig. 2(b)]. Thus the cluster geometries are not affected by heating to 378 K, and no isomerization occurs.

In summary, we have used ion mobility measurements to characterize the structure of gas-phase tin cluster cations. Up to about 35 atoms, they track the prolate growth pattern of silicon and especially germanium species rather than adding concentric atomic shells, although the exact size-dependent variations in mobility differ above $n \sim 20$. Starting from $n \sim 35$, tin clusters rearrange towards near-spherical geometries similar to those of Si and Ge. However, the structural transition is not abrupt like that for Si and Ge, but occurs in steps over a much wider size range, through a series of increasingly more compact structural families. Some of the clusters for $n \geqslant 18$ have two or more isomers. For all sizes studied, the observed geometries are stable, resistant to collisional excitation and to cooling or heating over a wide range of temperatures overlapping the region of $\alpha \Leftrightarrow \beta$ transformation in bulk tin. This is a report of a metal producing clusters with highly elongated shape.

We thank Dr. P. Jackson, Dr. L. Molina, Professor M. J. Stott, B. Wang, and Professor G. D. Willett for providing us with their optimized geometries of small tin clusters, and Professor K. M. Ho, Dr. Z. Y. Lu, and Dr. C. Z. Wang for useful discussions. This research was supported by the National Science Foundation and the U.S. Army Research Office.

[1] W. A. de Heer, Rev. Mod. Phys. **65**, 611 (1993).
[2] T. P. Martin, T. Bergmann, H. Göhlich, and T. Lange, J. Phys. Chem. **95**, 6421 (1991).
[3] B. J. Winter, T. D. Klots, E. K. Parks, and S. J. Riley, Z. Phys. D **19**, 375 (1991).
[4] T. D. Klots, B. J. Winter, E. K. Parks, and S. J. Riley, J. Chem. Phys. **92**, 2110 (1990); **95**, 8919 (1991).
[5] E. K. Parks, B. J. Winter, T. D. Klots, and S. J. Riley, J. Chem. Phys. **96**, 8267 (1992).
[6] E. K. Parks, L. Zhu, J. Ho, and S. J. Riley, Z. Phys. D **26**, 41 (1993).
[7] E. K. Parks, L. Zhu, J. Ho, and S. J. Riley, J. Chem. Phys. **100**, 7206 (1994).
[8] E. K. Parks, L. Zhu, J. Ho, and S. J. Riley, J. Chem. Phys. **102**, 7377 (1995).
[9] W. D. Knight, K. Clemenger, W. A. de Heer, W. A. Saunders, M. Y. Chou, and M. L. Cohen, Phys. Rev. Lett. **52**, 2141 (1984).
[10] M. F. Jarrold and J. E. Bower, J. Chem. Phys. **98**, 2399 (1993).
[11] M. F. Jarrold and J. E. Bower, J. Phys. Chem. **97**, 1746 (1993).
[12] M. Pellarin, B. Baguenard, C. Bordas, M. Broyer, J. Lerme, and J. L. Vialle, Phys. Rev. B **48**, 17 645 (1993).
[13] B. Baguenard, M. Pellarin, C. Bordas, J. Lerme, J. L. Vialle, and M. Broyer, Chem. Phys. Lett. **205**, 13 (1993).
[14] M. Pellarin, B. Baguenard, C. Bordas, M. Broyer, J. Lerme, and J. L. Vialle, Z. Phys. D **26**, S137 (1993).
[15] K. Rademann, M. Ruppel, and B. Kaiser, Ber. Bunsenges. Phys. Chem. **96**, 1204 (1992).
[16] T. P. Martin, T. Bergmann, H. Göhlich, and T. Lange, Z. Phys. D **19**, 25 (1991).
[17] B. Baguenard, M. Pellarin, J. Lerme, J. L. Vialle, and M. Broyer, J. Chem. Phys. **100**, 754 (1994).
[18] G. von Helden, M. T. Hsu, N. Gotts, and M. T. Bowers, J. Phys. Chem. **97**, 8182 (1993).
[19] M. F. Jarrold and V. A. Constant, Phys. Rev. Lett. **67**, 2994 (1991).
[20] M. F. Jarrold and J. E. Bower, J. Chem. Phys. **96**, 9180 (1992).
[21] J. M. Hunter, J. L. Fye, M. F. Jarrold, and J. E. Bower, Phys. Rev. Lett. **73**, 2063 (1994).
[22] K. M. Ho, A. A. Shvartsburg, B. Pan, Z. Y. Lu, C. Z. Wang, J. G. Wacker, J. L. Fye, and M. F. Jarrold, Nature (London) **392**, 582 (1998).
[23] B. Liu, Z. Y. Lu, B. Pan, C. Z. Wang, K. M. Ho, A. A. Shvartsburg, and M. F. Jarrold, J. Chem. Phys. **109**, 9401 (1998).
[24] A. A. Shvartsburg, M. F. Jarrold, B. Liu, Z. Y. Lu, C. Z. Wang, and K. M. Ho, Phys. Rev. Lett. **81**, 4616 (1998).
[25] W. G. Burgers and L. J. Groen, Discuss. Faraday Soc. **23**, 183 (1957).
[26] K. Gingerich, A. Desideri, and D. L. Cocke, J. Chem. Phys. **62**, 731 (1975).
[27] T. P. Martin and H. Schaber, J. Chem. Phys. **83**, 855 (1985).
[28] J. C. Phillips, J. Chem. Phys. **87**, 1712 (1987).
[29] M. Watanabe, Y. Saito, S. Nishigaki, and T. Noda, Jpn. J. Appl. Phys., Part 1 **27**, 344 (1988).
[30] Y. Saito and T. Noda, Z. Phys. D **12**, 225 (1989).
[31] K. LaiHing, R. G. Wheeler, W. L. Wilson, and M. A. Duncan, J. Chem. Phys. **87**, 3401 (1987).
[32] G. Gantefor, M. Gausa, K. H. Meiwes-Broer, and H. O. Lutz, Faraday Discuss. Chem. Soc. **86**, 197 (1988); Z. Phys. D **12**, 405 (1989).
[33] X. Ren and K. M. Ervin, Chem. Phys. Lett. **198**, 229 (1992).
[34] P. Jackson, I. G. Dance, K. J. Fisher, G. D. Willett, and G. E. Gadd, Int. J. Mass Spectrom. Ion Processes **157/158**, 329 (1996).
[35] A. B. Anderson, J. Chem. Phys. **63**, 4430 (1975).
[36] D. Dai and K. Balasubramanian, J. Chem. Phys. **96**, 8345 (1991); J. Phys. Chem. **96**, 9236 (1992); *ibid.* **100**, 19321

(1996); J. Chem. Phys. **108**, 4379 (1998).
[37] B. Wang, L. M. Molina, M. J. Lopez, A. Rubio, J. A. Alonso, and M. J. Stott, Ann. Phys. (Leipzig) **7**, 107 (1998).
[38] E. Honea, A. Ogura, C. A. Murray, K. Raghavachari, W. O. Sprenger, M. F. Jarrold, and W. L. Brown, Nature (London) **366**, 42 (1993).
[39] S. Li, R. J. Van Zee, W. Weltner, Jr., and K. Raghavachari, Chem. Phys. Lett. **243**, 275 (1995).
[40] C. Xu, T. R. Taylor, G. R. Burton, and D. M. Neumark, J. Chem. Phys. **108**, 1395 (1998).
[41] G. R. Burton, C. Xu, C. C. Arnold, and D. M. Neumark, J. Chem. Phys. **104**, 2757 (1996).
[42] J. R. Chelikowsky, S. Öğüt, X. Jing, K. Wu, A. Stathopoulos, and Y. Saad, in *Materials Theory, Simulations, and Parallel Algorithms*, edited by E. Kaxiras, J. Joannapoulos, P. Vashishta, and R. K. Kalia, MRS Symposia Proceedings No. 408 (Materials Research Society, Pittsburgh, 1996), p. 19.
[43] S. Öğüt and J. R. Chelikowsky, Phys. Rev. B **55**, R4914 (1997).
[44] I. Vasiliev, S. S. Öğüt, and J. R. Chelikowsky, Phys. Rev. Lett. **78**, 4805 (1997).
[45] P. Ballone, W. Andreoni, R. Car, and M. Parrinello, Phys. Rev. Lett. **60**, 271 (1988).
[46] M. F. Jarrold, J. Phys. Chem. **99**, 11 (1995).
[47] This calculation is performed using the exact hard spheres scattering (EHSS) model [48]. However, a sphere has no concave surface elements, so its EHSS collision integral equals [48] the orientationally averaged projection determined by the projection approximation [18]. The He collision radius of $R = 1.20$ Å was assumed.
[48] A. A. Shvartsburg and M. F. Jarrold, Chem. Phys. Lett. **261**, 86 (1996).
[49] Because of the upper limit of quadrupole mass spectrometer range equal to ~4000 amu [21], this transition has been followed for the doubly charged Ge_n cations. However, the structures of Ge_n^{2+} and Ge_n^{+} for the slightly smaller sizes ($n = 44-54$) are very similar [21]. We have also found that the structural transitions in Si_n^{2+} and Si_n^{+} take place over the exact same size range of $n = 26-34$ [A. A. Shvartsburg and M. F. Jarrold (unpublished)].
[50] A. A. Shvartsburg and M. F. Jarrold (unpublished). The conclusion [21] that the large Ge_n^{2+} clusters are not spherical preceded the development of sophisticated techniques [48,51,52] for the modeling of gas phase mobilities of polyatomic ions.
[51] M. F. Mesleh, J. M. Hunter, A. A. Shvartsburg, G. C. Schatz, and M. F. Jarrold, J. Phys. Chem. **100**, 16 082 (1996).
[52] A. A. Shvartsburg, G. C. Schatz, and M. F. Jarrold, J. Chem. Phys. **108**, 2416 (1998).
[53] K. Rademann, B. Kaiser, U. Even, and F. Hensel, Phys. Rev. Lett. **59**, 2319 (1987).
[54] C. Brechignac, M. Broyer, Ph. Cahuzac, G. Delacretaz, P. Labastie, J. P. Wolf, and L. Wöste, Phys. Rev. Lett. **60**, 275 (1988).
[55] H. Haberland, B. von Issendorff, J. Yufeng, and T. Kolar, Phys. Rev. Lett. **69**, 3212 (1992).
[56] M. E. Garcia, G. M. Pastor, and K. H. Bennemann, Phys. Rev. Lett. **67**, 1142 (1991).
[57] The collision integrals of all species are inversely correlated with buffer gas temperature. In calculations, this can be crudely accounted for via a temperature-dependent He collision radius [58,59]. When evaluating the cross sections for spheres at 78 and 378 K, we have adjusted R so that the values for the smallest ($n \leqslant 10$) clusters, the mobilities of which are only weakly sensitive to geometry [22,23], would match those found at 305 K. This has produced $R = 2.04$ Å at 78 K and 1.09 Å at 378 K (assuming the bulk density of β-tin).
[58] T. Wyttenbach, G. von Helden, and M. T. Bowers, J. Am. Chem. Soc. **118**, 8355 (1996).
[59] S. Lee, T. Wyttenbach, and M. T. Bowers, Int. J. Mass Spectrom. Ion Processes **167/168**, 605 (1997).
[60] A. A. Shvartsburg, B. Liu, Z. Y. Lu, C. Z. Wang, M. F. Jarrold, and K. M. Ho (unpublished).
[61] For larger clusters, the values at 305 K appear to be slightly higher. It is not clear at this juncture if this carries any structural information. It might be due to a marginal thermal annealing.